World Journal of

Gastroenterology

World Journal of Gastroenterology

Contents

Contents

Contents

ABOUT COVER

Editorial Board Member of *World Journal of Gastroenterology*, Veerapol Kukongviriyapan, PhD, Professor, Department of Pharmacology, Faculty of Medicine, Khon Kaen University, 123 Moo 16, Mittraphap Road, Muang District, Khon Kaen 40002, Thailand. veerapol@kku.ac.th

AIMS AND SCOPE

The primary aim of *World Journal of Gastroenterology* (*WJG*, *World J Gastroenterol*) is to provide scholars and readers from various fields of gastroenterology and hepatology with a platform to publish high-quality basic and clinical research articles and communicate their research findings online. *WJG* mainly publishes articles reporting research results and findings obtained in the field of gastroenterology and hepatology and covering a wide range of topics including gastroenterology, hepatology, gastrointestinal endoscopy, gastrointestinal surgery, gastrointestinal oncology, and pediatric gastroenterology.

INDEXING/ABSTRACTING

The *WJG* is now indexed in Current Contents®/Clinical Medicine, Science Citation Index Expanded (also known as SciSearch®), Journal Citation Reports®, Index Medicus, MEDLINE, PubMed, PubMed Central, and Scopus. The 2021 edition of Journal Citation Report® cites the 2020 impact factor (IF) for *WJG* as 5.742; Journal Citation Indicator: 0.79; IF without journal self cites: 5.590; 5-year IF: 5.044; Ranking: 28 among 92 journals in gastroenterology and hepatology; and Quartile category: Q2. The *WJG*'s CiteScore for 2020 is 6.9 and Scopus CiteScore rank 2020: Gastroenterology is 19/136.

RESPONSIBLE EDITORS FOR THIS ISSUE

Production Editor: *Ji-Hong Liu*; **Production Department Director:** *Yu-Jie Ma*; **Editorial Office Director:** *Ze-Mao Gong*.

ORIGINAL ARTICLE

Retrospective Study

Magnetic resonance imaging-radiomics evaluation of response to chemotherapy for synchronous liver metastasis of colorectal cancer

Yan-Qing Ma, Yang Wen, Hong Liang, Jian-Guo Zhong, Pei-Pei Pang

ORCID number: Yan-Qing Ma 0000-0002-6131-3284; Yang Wen 0000-0003-3961-4328; Hong Liang 0000-0003-1598-2409; Jian-Guo Zhong 0000-0001-6344-2883; Pei-Pei Pang 0000-0001-9318-6315.

Yan-Qing Ma, Yang Wen, Jian-Guo Zhong, Department of Radiology, Zhejiang Provincial People's Hospital, Affiliated People's Hospital of Hangzhou Medical College, Hangzhou 310000, Zhejiang Province, China

Hong Liang, Department of Radiology, Hangzhou Medical College, Hangzhou 310000, Zhejiang Province, China

Pei-Pei Pang, Department of Pharmaceuticals Diagnosis, GE Healthcare, Hangzhou 310000, Zhejiang Province, China

Corresponding author: Yang Wen, MD, Chief Doctor, Department of Radiology, Zhejiang Provincial People's Hospital, Affiliated People's Hospital of Hangzhou Medical College, No. 158 Shangtang Road, Hangzhou 310000, Zhejiang Province, China. 13989454104@163.com

Abstract

BACKGROUND
Synchronous liver metastasis (SLM) is an indicator of poor prognosis for colorectal cancer (CRC). Nearly 50% of CRC patients develop hepatic metastasis, with 15%-25% of them presenting with SLM. The evaluation of SLM in CRC is crucial for precise and personalized treatment. It is beneficial to detect its response to chemotherapy and choose an optimal treatment method.

AIM
To construct prediction models based on magnetic resonance imaging (MRI)-radiomics and clinical parameters to evaluate the chemotherapy response in SLM of CRC.

METHODS
A total of 102 CRC patients with 223 SLM lesions were identified and divided into disease response (DR) and disease non-response (non-DR) to chemotherapy. After standardizing the MRI images, the volume of interest was delineated and radiomics features were calculated. The MRI-radiomics logistic model was constructed after methods of variance/Mann-Whitney *U* test, correlation analysis, and least absolute shrinkage and selection operator in feature selecting. The radiomics score was calculated. The receiver operating characteristics curves by the DeLong test were analyzed with MedCalc software to compare the validity of all models. Additionally, the area under curves (AUCs) of DWI, T2WI, and portal phase of contrast-enhanced sequences radiomics model (Ra-DWI, Ra-T2WI, and

Ra-portal phase of contrast-enhanced sequences) were calculated. The radiomics-clinical nomogram was generated by combining radiomics features and clinical characteristics of CA19-9 and clinical N staging.

RESULTS
The AUCs of the MRI-radiomics model were 0.733 and 0.753 for the training (156 lesions with 68 non-DR and 88 DR) and the validation (67 lesions with 29 non-DR and 38 DR) set, respectively. Additionally, the AUCs of the training and the validation set of Ra-DWI were higher than those of Ra-T2WI and Ra-portal phase of contrast-enhanced sequences (training set: 0.652 *vs* 0.628 and 0.633, validation set: 0.661 *vs* 0.575 and 0.543). After chemotherapy, the top four of twelve delta-radiomics features of Ra-DWI in the DR group belonged to gray-level run-length matrices radiomics parameters. The radiomics-clinical nomogram containing radiomics score, CA19-9, and clinical N staging was built. This radiomics-clinical nomogram can effectively discriminate the patients with DR from non-DR with a higher AUC of 0.809 (95% confidence interval: 0.751-0.858).

CONCLUSION
MRI-radiomics is conducive to predict chemotherapeutic response in SLM patients of CRC. The radiomics-clinical nomogram, involving radiomics score, CA19-9, and clinical N staging is more effective in predicting chemotherapeutic response.

Key Words: Radiomics; Synchronous liver metastasis; Colorectal cancer; Chemotherapy; Magnetic resonance; Nomogram

Core Tip: Synchronous liver metastasis (SLM) indicates poor prognosis for colorectal cancer. Nearly 50% of colorectal cancer patients develop hepatic metastasis, with 15%-25% of them presenting with SLM. It is beneficial to detect the response of SLM to chemotherapy. Magnetic resonance imaging-radiomics could provide a non-invasive approach to predict the risk of SLM. The logistic model of DWI sequence behaved the best in evaluating the chemotherapeutic response in SLM compared with T2WI, DWI, and portal phase of contrast-enhanced sequences. Moreover, the radiomics-clinical nomogram containing radiomics score, CA19-9, and clinical N staging is more effective in predicting the chemotherapeutic response of SLM patients.

INTRODUCTION

Colorectal cancer (CRC) is the fourth most common malignancy worldwide[1], accounting for approximately one-third of cancer related deaths in western countries [2]. Nearly 50% of CRC patients developed hepatic metastasis throughout the course of disease, and 15%-25% of them were associated synchronous liver metastasis (SLM) [3]. SLM is confirmed as an indicator of poor prognosis for CRC, which was defined as a lesion identified within 90 d after the diagnosis of the primary tumor[4]. Currently, the standard guideline for the treatment of CRC patients with SLM remains undetermined. Conventional treatment for this condition is colectomy, followed by chemotherapy and liver resection[5]. Preoperative chemotherapy has superiority on early treatment of metastatic disease, which may help to achieve a negative resection margin[6] and reduce the risk of local recurrence[1]. However, liver injuries can be induced by chemotherapy, such as vascular changes and chemotherapy-associated steatohepatitis[7]. Previous studies have reported that administration of more than 12

cycles of preoperative chemotherapy increased the risk of re-operation and prolonged hospital stay[8]. Excessive cycles of preoperative chemotherapy may result in increased damage to the liver and lost potential opportunity to receive surgery[7] since progression of chemotherapy is irreversible. Therefore, precise and non-invasive assessment of the response of SLM patients to preoperative chemotherapy is a critical step in individualized treatment. In addition, SLM patients who were predicted as non-responders could benefit from alternative therapies to avoid dispensable chemotherapy.

Radiomics is a promising and non-invasive method to analyze conventional imaging features and incorporate them into predictive models to evaluate tumor behaviors[9]. Previous work has concluded that the nomogram combining radiomics and clinical factors exhibited favorable ability and accuracy in evaluating metastatic pulmonary nodules in CRC patients[10]. Analysis of liver texture is potentially a supplement to routine computed tomography examination and may provide prognostic markers for CRC patients[11]. A radiomics signature was validated to be a complementary predictor for preoperative staging of CRC patients[12]. It has been suggested that magnetic resonance imaging (MRI)-radiomics of CRC patients could provide a non-invasive approach to predict the risk of SLM[13].

To the best of our knowledge, little attention has been paid to predict the response of chemotherapy in SLM patients. This retrospective study examined the emerging role of MRI-radiomics signature in order to detect the prediction efficiency of models in chemotherapeutic response of SLM patients and avoid ineffective chemotherapy.

MATERIALS AND METHODS

Patient selection

This retrospective study was approved by the institutional review board of our hospital. For the characteristics of retrospective study, formal written consent is not applicable. Research methods were carried out in accordance with the Declaration of Helsinki.

A total of 102 CRC patients with 223 SLM lesions were identified from 2017 to 2020 in our hospital. SLM was a histopathologically confirmed intrahepatic lesion within 90 d of the diagnosis of CRC[4]. Inclusion criteria included: (1) Patients were histopathologically diagnosed as classical adenocarcinoma in CRC, excluding mucinous and signet ring adenocarcinoma[14]; (2) Patients have at least one SLM lesion; (3) For patients with multiple SLM lesions, the top three largest ones were selected to analyze; (4) Patients underwent baseline and 3 mo follow-up MRI examination after the start of chemotherapy; and (5) Patients underwent mFOLFOX7 chemotherapy regimen. Exclusion criteria included: (1) Patients underwent anti-tumor treatments such as chemotherapy, radiotherapy, or transarterial chemoembolization before baseline MRI examinations; (2) Patients were diagnosed with CRC with biopsy but not with surgery; (3) History of other malignancies; and (4) Patients were diagnosed as mucinous or signet ring adenocarcinoma. The general characteristics involved gender, age, tumor markers, and clinical T/N staging were recorded. The tumor markers encompassed alpha-fetoprotein (normal range: 0.0-20.0 μg/L), carcinoembryonic antigen (normal range: 0.0-5.0 μg/L), and CA19-9 (normal range: 0.0-37.0 U/mL) that all were divided into normal and abnormal subgroups.

The response to chemotherapy was assessed after 3 mo from the start of chemotherapy by MRI examinations. The response of lesions was categorized into four subgroups according to the Response Evaluation Criteria in Solid Tumors (version 1.1) criterion[15]: (1) Complete response refers that all target lesions disappeared; (2) Partial response is defined as lesions having at least a 30% decrease in the sum diameters of lesions; (3) Progressive disease is defined as lesions having at least a 20% increase in the sum diameters of lesions; and (4) Stable disease is defined as tumors with neither sufficient shrinkage nor sufficient increase in the lesions. None of the patients in this study belonged to complete response. Patients with partial response were classified as disease response (DR) group (Figure 1), while patients with progressive or stable disease were merged into disease non-response (non-DR) group.

MRI examination and image processing

All examinations were performed using 3.0-T MRI (Discovery 750, GE Healthcare, Waukesha, WI, United States). The axial T2WI, DWI, and portal phase of contrast-enhanced sequences (CE_{PP}) were taken. CE-MRI was performed with gadobenate dimeglumine being injected *via* a dual head pressure injector at a rate of 2 mL/s and
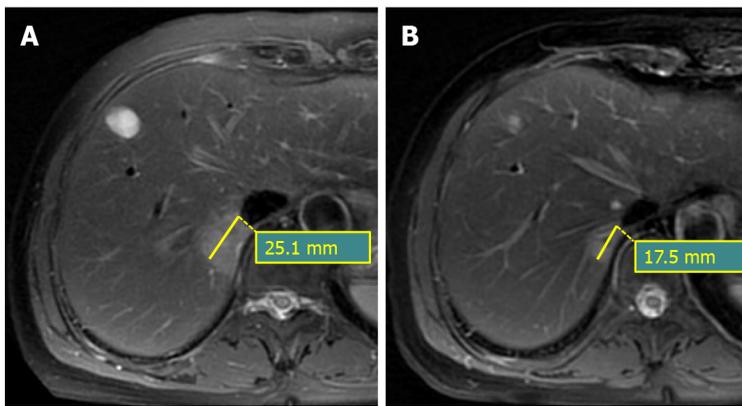
Figure 1 Magnetic resonance imaging examinations. A: A 48-year-old female had a synchronous liver metastasis with baseline long diameter of 25.1 mm; B: After chemotherapy, the lesion a had 30.3% decrease in long diameter of 17.5 mm, which belonged to the disease response group for analysis.

followed by 20 mL saline flush at the same rate. Post-contrast image acquisition was done in the axial plane in arterial phase (AP), PP, and equilibrium phases (EP). The imaging parameters were as follows: T2WI (TR 10000-12000 ms, TE 85 ms; FOV 36 cm × 40 cm, matix 320 × 320, thickness 5.0 mm, interval 1.0 mm), CE (TR 3.7 ms, TE 2.2 ms; FA 12°, matix 260 × 260, thickness 5.0 mm, interval 1.0 mm, 0.2 mL/Kg), and DWI (TR 3500 ms, TE 75 ms; FOV 32 cm × 32 cm, matix 128 × 128, thickness 3.0 mm, interval 0.6 mm, *b* value 0 and 800 s/mm²).

The process of image standardization included resampling images into a 1.0 mm × 1.0 mm × 1.0 mm voxel size of X/Y/Z-spacing, denoising images by Gaussian, and normalizing the gray level of images to a scale from 1 to 32, which is automatically performed with the software of AK (Artificial Intelligence Kit, version 3.0.0, GE Healthcare).

Then, the three-dimensional volume of interest (VOI) was manually delineated in all the images by software of "ITK-SNAP" (version 3.4.0, http://www.itksnap.org/) by two radiologists with 9 and 12 years of experience in MRI diagnosis, respectively. Finally, the radiomics features of two radiologists were automatically calculated in AK software.

MRI-radiomics signature construction

A total of 396 radiomics features were automatically calculated by AK software, including 42 histogram parameters, 54 texture parameters, 9 form factor parameters, 100 gray-level co-occurrence matrices parameters, 180 gray-level run-length matrices parameters (RLM), and 11 gray-level size zone matrices parameters. The specific description of radiomics features is presented in the Supplemental Material. These radiomics features have underlying relationships with pathophysiological characteristics[16], intracellular heterogeneity[17], as well as genotypes[18], and so on.

Five steps were carried out to select radiomics features. First, the intra-class correlation coefficient (ICC) for all features by two radiologists was analyzed. Features with ICC greater than 0.80 were selected[19], and the mean values of radiomics features from two radiologists were calculated as robust features for further analysis. Second, we normalized the selected radiomics features by replacing the abnormal values with mean and converting the features into non-dimensional values *via* subtracting by mean and dividing by standard deviation value to eliminate discrepancies. Third, we randomly grouped the cohort into a training set and a validation set with a proportion of 7:3 (156 lesions in the training set with 68 non-DR and 88 DR lesions, 67 lesions in the validation set with 29 non-DR and 38 DR lesions). Fourth, we applied analysis of variance/Mann-Whitney *U* test, correlation analysis, and least absolute shrinkage and selection operator to select optimal features. The specific explanation of the methods to select radiomics features is summarized in the Supplemental Material. Last, the MRI-radiomics logistic model to differentiate DR and non-DR patients was constructed in the training set and verified by the validation set. The workflow of the radiomics signature in differentiating DR and non-DR patients was illustrated in Figure 2.

The calibration curves were depicted to compare the consistency between predicted and actual ability to evaluate response to chemotherapy, accompanied by Hosmer-Lemeshow test. The receiver operating characteristic curve was constructed by DeLong test, and the area under curve (AUC) was calculated to evaluate the validity of
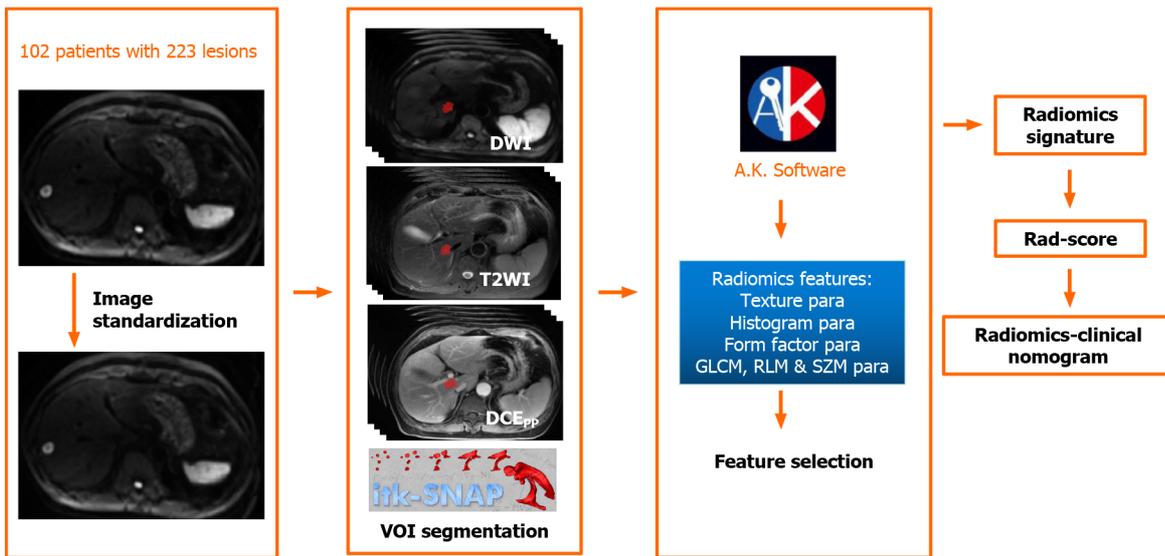
Figure 2 The workflow of radiomics signature in differentiating the responses of synchronous liver metastasis patients to chemotherapy. VOI: Volume of interest; GLCM: Gray-level co-occurrence matrices; RLM: Run-length matrices; SZM: Size zone matrices; Rad-score: Radiomics score.

MRI-radiomics logistic models.

Statistical analysis

Analysis of variance/Mann-Whitney *U* test /MW, correlation analysis, least absolute shrinkage and selection operator, the logistic model construction, the calibration curve establishment, and radiomics-clinical nomogram development were performed with R software V4.0.1 to select features that potentially predict chemotherapeutic response. The calibration curves were depicted with Hosmer-Lemeshow test to compare the consistency between predicted and actual ability of evaluating response of chemotherapy. The receiver operating characteristic curves were constructed to calculate the AUC with a 95% confidence interval (CI), and the DeLong test was made to evaluate the validity of models in MedCalc V18.2.1. The general information, such as gender, age, tumor index, and T/N stage, was analyzed with IBM SPSS V22.0, using χ^2 or independent samples *t*-test. A two-tailed *P* < 0.05 was considered statistically significant.

RESULTS

Patients' general information

General information of patients were listed in Table 1. A total of 102 patients with 223 lesions were enrolled. There were 53 patients with 97 lesions in the non-DR group and 49 patients with 126 lesions in the DR group. The mean age of non-DR was 63.2 ± 9.5-years-old, and that of DR was 59.9 ± 11.6-years-old. In general, baseline demographics and tumor characteristics were balanced in the DR and non-DR groups, with exceptions of CA19-9 (*P* = 0.045) and clinical N staging (*P* = 0.030). Higher ratios of patients with normal CA19-9 levels were enrolled in the non-DR group (non-DR was 56.6% *vs* DR was 36.7%). In regard to clinical N staging, patients in the non-DR group primarily were staged to be N1 (52.8%), while stage N2 (73.5%) ranked the top in the DR group.

MRI-radiomics logistic model construction

Among the total 1188 radiomics features from T2WI, DWI, and CE$_{PP}$ sequences of MRI examination, 893 features with ICC greater than 0.80 between two radiologists remained for the following analysis. After decreasing redundant features with the methods of analysis of variance/Mann-Whitney *U* test, correlation analysis, and least absolute shrinkage and selection operator, 12 features were selected to construct the MRI-radiomics logistic model for predicting responses of chemotherapy (Figure 3) and the radiomics score (rad-score) was calculated accordingly. The 12 optimal features included four DWI features , six T2WI features , and two CE$_{PP}$ features. The AUC of

Table 1 Baseline patient characteristics

General characteristics	non-DR, *n* = 53	DR, *n* = 49	*P* value
Demographics			
Gender (female/male)	28/25	17/32	0.065
Age (mean ± SD)	63.3 ± 11.1/63.2 ± 7.5	58.6 ± 11.2/59.7 ± 14.1	0.117
Tumor markers			
AFP (normal/abnormal)	51/2	47/2	0.936
CEA (normal/abnormal)	14/39	14/35	0.807
CA19-9 (normal/abnormal)	30/23	18/31	0.045
Clinical T/N staging			
T1/T2/T3/T4	0/1/48/4	0/10/33/6	0.136
N0/N1/N2	3/28/22	5/8/36	0.030

The characteristics of age and clinical T/N staging were analyzed by independent-samples *t*-test. The data of gender and tumor markers of AFP/CEA/CA19-9 were analyzed by Pearson χ^2. A *P* < 0.05 was viewed as statistically significant. Non-DR: Disease non-response group; DR: Disease response group; SD: Standard deviation; AFP: Alpha-fetoprotein; CEA: Carcinoembryonic antigen.
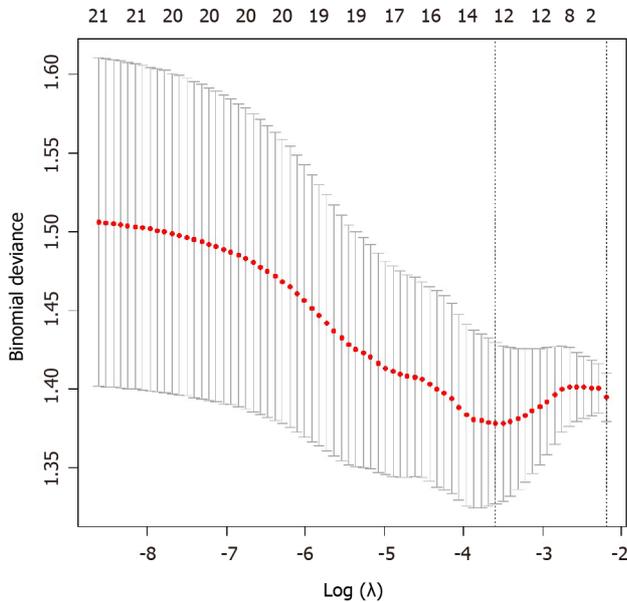
Figure 3 The feature selection method of least absolute shrinkage and selection operator. A total of 12 optimal features were selected.

this model was 0.733 (95%CI, 0.656-0.800) in the training set and was 0.753 (95%CI, 0.633-0.849) in the validation set. The calibration curves showed good consistency in the predicted and the actual ability to evaluate chemotherapy responses in both training and validation sets. The non-significant Hosmer-Lemeshow test suggested goodness-of-fit for the MRI-radiomics logistic models in the training (*P* = 0.858) and validation (*P* = 0.374) set.

Furthermore, we also compared prediction efficiency in chemotherapeutic response between different radiomics models of single DWI, T2WI, or CE$_{PP}$ sequence (Ra-DWI, Ra-T2WI, Ra-CE$_{PP}$). The AUCs of these models were listed in Table 2. The AUCs of the training set and validation set of Ra-DWI were 0.652 (95%CI, 0.571-0.726) and 0.661 (95%CI, 0.536-0.772), which were higher than those of Ra-T2WI and Ra-CE$_{PP}$ (Table 2). Then we compared the radiomics features of DWI between the baseline and after chemotherapy in the DR group. There were 105 lesions enrolled, as the post-chemotherapy images of another 21 lesions were not satisfactory. By features selection, 11 significant delta-radiomics features were left. The remaining features included histogram (Quantile 0.025), texture (ClusterShade_angle90_offset1), gray-level co-occurrence matrices Entropy (GLCMEntropy_angle135_offset7/_angle90_offset1, and

Table 2 The area under the curve of radiomics model of DWI sequence, radiomics model of T2WI sequence, and radiomics model of portal phase of contrast-enhanced sequences models in the training set and the validation set

Sequence	Training set	*P* value	Validation set	*P* value
Ra-DWI	0.652 (95%CI, 0.571-0.726)	0.001	0.661 (95%CI, 0.536-0.772)	0.018
Ra-T2WI	0.628 (95%CI, 0.547-0.704)	0.005	0.575 (95%CI, 0.450-0.695)	0.291
Ra-CE$_{PP}$	0.633 (95%CI, 0.552-0.709)	0.003	0.543 (95%CI, 0.418-0.664)	0.544

A *P* < 0.05 of the DeLong test was considered statistically significant. The DeLong test of validation set in radiomics model of T2WI sequence and radiomics model of portal phase of contrast-enhanced sequences had no statistical significance. Ra-DWI: Radiomics model of DWI sequence; Ra-T2WI: Radiomics model of T2WI sequence; Ra-CE$_{PP}$: Radiomics model of portal phase of contrast-enhanced sequences; CI: Confidence interval.

differenceEntropy), RLM (LongRunHighGreyLevelEmphasis_AllDirection_offset1_SD/_angle45_offset7, ShortRun Emphasis_angle45/90_offset1/HighGrey-LevelEmphasis_angle90_offset7), and size zone variability. The top 4 of the 11 delta-radiomics features belonged to RLM parameters.

Radiomics-clinical nomogram analysis

For clinical characteristics, tumor marker CA19-9 (*P* = 0.045) and clinical N staging (*P* = 0.030) were demonstrated to be statistically different between DR and non-DR groups. Thus, CA19-9 and clinical N staging, together with rad-score were integrated into the logistic model to construct the radiomics-clinical nomogram (Figure 4). The formula of the logistic model was: Y = -2.141 + 1.018 × [rad-score] + 0.893 × [CA19-9] + 1.042 × [N staging]. The AUC of the radiomics-clinical nomogram was 0.809 (95%CI, 0.751-0.858).

DISCUSSION

The standardized treatment for SLM patients is unascertained, and early detection of patients with DR or non-DR is crucial for personalized treatment planning. In order to predict patients' responses to chemotherapy, we generated a MRI-radiomics based model in this study. The AUC of this model was 0.733 in the training set and was 0.753 in the validation set. Non-significant Hosmer-Lemeshow test and the calibration curve of the MRI-radiomics model showed good consistency between the predicted and actual probability. Although the AUC value was not ideal enough, the non-invasive MRI examination is still beneficial to differentiate non-DR and DR in clinical practice. There were 156 lesions with 68 non-DR and 88 DR lesions in the training set and 12 radiomics features to construct MR-radiomics logistic model. The sample size of the logistic model often relies on an events per predictor variable[20]. Vittinghoff *et al*[21] conducted a large simulation study of other influences on relative bias, confidence interval coverage, and type I error and found that the events per predictor variable between 5 to 9 could achieve acceptable results. In our study, the events per predictor variable were 5.7 in non-DR group and were 7.3 in the DR group, which were both in the range of 5 to 9. Therefore we believed that the MRI-radiomics model based on 156 lesions in the training set was valid.

As for the selection of MRI sequences, a recent investigation in reproducibility and robustness of MRI radiomics has suggested that caution should be taken in the interpretation of clinical studies using T1WI features to delineate VOI[22]. Meanwhile, after making some attempt in the exploration stage, we realized that it was difficult and inaccurate to depict VOI in AP and EP of CE sequence. Thus, we selected DWI, T2WI, and PP of CE sequences to do future research. Features with ICC more than 0.80 identified by two radiologists were selected, and the mean values of selected features were calculated as robust features for further analysis. After comparing the predictive efficiency between Ra-DWI, Ra-T2WI, and Ra-CE$_{PP}$, Ra-DWI demonstrated out-standing predictive value compared with Ra-T2WI and Ra-CE$_{PP}$ (AUCs in the training set: 0.652 *vs* 0.628, 0.633; AUCs in the validation set: 0.661 *vs* 0.575, 0.543). We should think highly of DWI due to its potential for evaluating DR and non-DR in clinical practice. As has been investigated that delta-radiomics analysis explored the change of radiomics features between baseline and follow-up computed tomography images can improve the differentiation of pre-invasive ground glass nodules from invasive ground glass nodules[23].
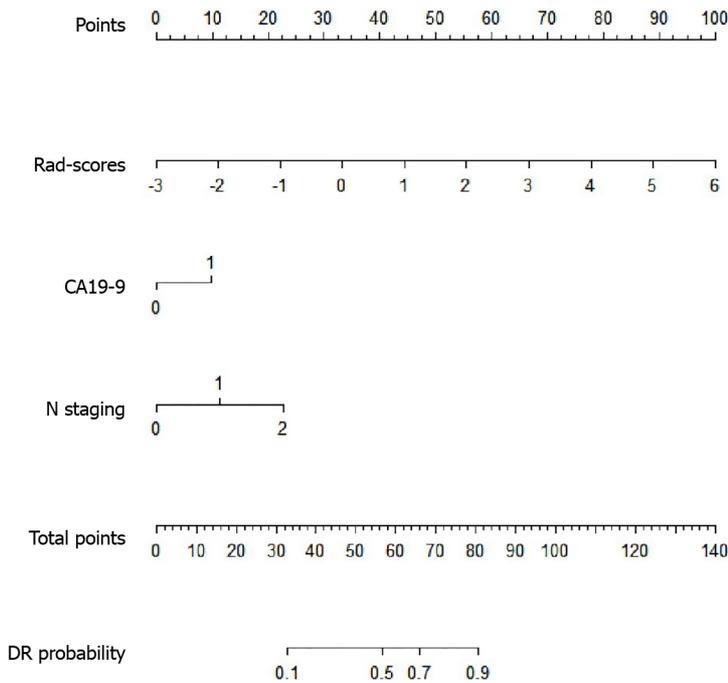
Figure 4 The nomogram of radiomics-clinical analysis to differentiate patients with disease non-response group from disease response group. The zero in CA19-9 represented normal and one referred to abnormal. DR: Disease response group; Rad-score: Radiomics score.

After comparing the delta-radiomics of DR between baseline and post-chemotherapy MRI examination, we obtained the top 4 of 11 delta-radiomics features of post-chemotherapy belonging to RLM parameters. Kim *et al*[24] analyzed the association between pathological characteristics and gray-level run-length matrices features of pancreatic cancer and revealed that gray-level non-uniformity values of RLM were powerful indicators for prognosis. RLM is more sensitive to reflect changes of regional heterogeneity since it analyzes radiomics changes through the whole length of the run [25]. These results suggested that DWI helped to discriminate patients with DR from non-DR in clinical practice.

The nomogram of incorporated independent risk factors for clinical events, such as differentiation[26], survival[27], and recurrence[28], has been widely applied in the field of oncology. The radiomics-clinical nomogram contained rad-score, CA19-9, and clinical N staging demonstrated better predictive accuracy compared with MRI-radiomics signature (AUC: 0.809 *vs* 0.733 in the training set, and 0.753 in the validation set). In patients with SLM, elevation of CA19-9 and carcinoembryonic antigen is a prognostic indicator and can predict response to treatment[29]. A previous study identified that CA19-9 was the best prognostic indicator of metastatic CRC[30] and also was a significant prognostic indicator for CRC patients treated with neoadjuvant chemoradiotherapy[29]. Similar to a previous study[31], we demonstrated that more patients (63.3%) with DR had elevated levels of CA19-9 than those with non-DR (43.4%), suggesting that CA19-9 was a promising indicator for predicting response to chemotherapy ($P < 0.05$). A study by Märkl *et al*[32] illustrated that lymph node staging played a significant role in prognosis evaluation and treatment stratification for CRC. In the current study, we confirmed that clinical N staging had a correlation to chemotherapeutic response. Taken together, the proposed radiomics-clinical nomogram is beneficial in estimating the chemotherapeutic response and in selecting appropriate patients to receive chemotherapy.

Our study had several limitations. First, we only took PP of CE for analysis since the lesions in AP and EP of CE sequence were not visible enough for VOI segmentation. An automatic segmentation method to deal with the AP/EP images remains to be developed. Second, this is a single center study, and the prediction models should be further verified in other centers and in a larger cohort. Third, the inevitable flaw may occur in this retrospective study since the histopathological grade and clinical characteristics of selected patients may be unbalanced. Fourth, as for the criteria for evaluating the response of chemotherapy, we chose the Response Evaluation Criteria in Solid Tumors criterion instead of considering histopathological evidence, which may be complementary to the results of the radiomics. Therefore, our results should be further validated in future multiangle and multiclassification sample studies.

CONCLUSION

In conclusion, our study indicated that the MRI-radiomics logistic model was a helpful and non-invasive predictor for differentiating patients with non-DR from DR. Ra-DWI was more efficient in distinguishing patients with non-DR from DR than that of Ra-T2WI and Ra-CE$_{PP}$, and the RLM parameter of Ra-DWI was superior in reflecting the delta-radiomics after chemotherapy. Furthermore, the radiomics-clinical nomogram based on the MRI-radiomics signature and clinical factors of CA19-9 and clinical N staging is conducive to better predict non-DR and DR of SLM patients and provides a theoretical and practical basis for the choice of treatment strategies.

ARTICLE HIGHLIGHTS

Research background

Synchronous liver metastasis (SLM) frequently occurs in colorectal cancer (CRC). Nearly 50% of CRC patients develop hepatic metastasis, with 15%-25% of them presenting with SLM. The evaluation of SLM in CRC is crucial for a precise and personalized treatment.

Research motivation

To construct prediction models based on magnetic resonance imaging (MRI)-radiomics and clinical parameters to evaluate the chemotherapy response in SLM patients in the context of CRC.

Research objectives

A total of 102 patients with 223 SLM lesions were identified and divided into disease response (DR) and disease non-response (non-DR) to chemotherapy.

Research methods

The MRI-radiomics logistic models containing T2WI, DWI, and portal phase of dynamic contrast-enhanced sequences radiomics models (Ra-T2WI, Ra-DWI and Ra-portal phase of dynamic contrast-enhanced sequences) were constructed after methods of feature dimension, and the respective radiomics score was calculated. Then radiomics-clinical nomogram was generated by combining radiomics score, CA19-9, and clinical N staging.

Research results

The AUCs of the training and validation set of Ra-DWI were 0.652 and 0.661, which were higher than those of Ra-T2WI and Ra-portal phase of dynamic contrast-enhanced sequences. After chemotherapy, the top four delta-radiomics features of Ra-DWI in DR group belonged to gray-level run-length matrices parameters. The radiomics-clinical nomogram was built with an AUC of 0.809 and can effectively discriminate the patients with DR from non-DR.

Research conclusions

MRI-radiomics is conducive to predict chemotherapeutic response in SLM patients. The Ra-DWI logistic model behaved the best in differentiating DR and non-DR. Run-length matrices parameters of Ra-DWI were more sensitive to reflect the delta-radiomics after chemotherapy. The radiomics-clinical nomogram is more effective in predicting chemotherapeutic response.

Research perspectives

This study provides new insights into the potential ability of MRI-radiomics in evaluating chemotherapeutic response in SLM patents. The MRI-radiomics features combined with clinical characteristics is more effective in evaluation.

REFERENCES

1   **Song JH**, Jeong JU, Lee JH, Kim SH, Cho HM, Um JW, Jang HS; Korean Clinical Practice Guideline for Colon and Rectal Cancer Committee. Preoperative chemoradiotherapy *vs* postoperative chemoradiotherapy for stage II-III resectable rectal cancer: a meta-analysis of randomized controlled

trials. *Radiat Oncol J* 2017; **35**: 198-207 [PMID: 29037017 DOI: 10.3857/roj.2017.00059]

2   **Siegel RL**, Miller KD, Jemal A. Cancer Statistics, 2017. *CA Cancer J Clin* 2017; **67**: 7-30 [PMID: 28055103 DOI: 10.3322/caac.21387]

3   **Manfredi S**, Lepage C, Hatem C, Coatmeur O, Faivre J, Bouvier AM. Epidemiology and management of liver metastases from colorectal cancer. *Ann Surg* 2006; **244**: 254-259 [PMID: 16858188 DOI: 10.1097/01.sla.0000217629.94941.cf]

4   **Conrad C**, Vauthey JN, Masayuki O, Sheth RA, Yamashita S, Passot G, Bailey CE, Zorzi D, Kopetz S, Aloia TA, You YN. Individualized Treatment Sequencing Selection Contributes to Optimized Survival in Patients with Rectal Cancer and Synchronous Liver Metastases. *Ann Surg Oncol* 2017; **24**: 3857-3864 [PMID: 28929463 DOI: 10.1245/s10434-017-6089-7]

5   **Tsoulfas G**, Pramateftakis MG. Management of rectal cancer and liver metastatic disease: which comes first? *Int J Surg Oncol* 2012; **2012**: 196908 [PMID: 22778934 DOI: 10.1155/2012/196908]

6   **Gall TM**, Basyouny M, Frampton AE, Darzi A, Ziprin P, Dawson P, Paraskeva P, Habib NA, Spalding DR, Cleator S, Lowdell C, Jiao LR. Neoadjuvant chemotherapy and primary-first approach for rectal cancer with synchronous liver metastases. *Colorectal Dis* 2014; **16**: O197-O205 [PMID: 24344746 DOI: 10.1111/codi.12534]

7   **Nordlinger B**, Benoist S. Benefits and risks of neoadjuvant therapy for liver metastases. *J Clin Oncol* 2006; **24**: 4954-4955 [PMID: 17075112 DOI: 10.1200/JCO.2006.07.9244]

8   **Aloia T**, Sebagh M, Plasse M, Karam V, Lévi F, Giacchetti S, Azoulay D, Bismuth H, Castaing D, Adam R. Liver histology and surgical outcomes after preoperative chemotherapy with fluorouracil plus oxaliplatin in colorectal cancer liver metastases. *J Clin Oncol* 2006; **24**: 4983-4990 [PMID: 17075116 DOI: 10.1200/JCO.2006.05.8156]

9   **Alahmari SS**, Cherezov D, Goldgof D, Hall L, Gillies RJ, Schabath MB. Delta Radiomics Improves Pulmonary Nodule Malignancy Prediction in Lung Cancer Screening. *IEEE Access* 2018; **6**: 77796-77806 [PMID: 30607311 DOI: 10.1109/ACCESS.2018.2884126]

10   **Hu T**, Wang S, Huang L, Wang J, Shi D, Li Y, Tong T, Peng W. A clinical-radiomics nomogram for the preoperative prediction of lung metastasis in colorectal cancer patients with indeterminate pulmonary nodules. *Eur Radiol* 2019; **29**: 439-449 [PMID: 29948074 DOI: 10.1007/s00330-018-5539-3]

11   **Miles KA**, Ganeshan B, Griffiths MR, Young RC, Chatwin CR. Colorectal cancer: texture analysis of portal phase hepatic CT images as a potential marker of survival. *Radiology* 2009; **250**: 444-452 [PMID: 19164695 DOI: 10.1148/radiol.2502071879]

12   **Liang C**, Huang Y, He L, Chen X, Ma Z, Dong D, Tian J, Liang C, Liu Z. The development and validation of a CT-based radiomics signature for the preoperative discrimination of stage I-II and stage III-IV colorectal cancer. *Oncotarget* 2016; **7**: 31401-31412 [PMID: 27120787 DOI: 10.18632/oncotarget.8919]

13   **Shu Z**, Fang S, Ding Z, Mao D, Cai R, Chen Y, Pang P, Gong X. MRI-based Radiomics nomogram to detect primary rectal cancer with synchronous liver metastases. *Sci Rep* 2019; **9**: 3374 [PMID: 30833648 DOI: 10.1038/s41598-019-39651-y]

14   **Nitsche U**, Zimmermann A, Späth C, Müller T, Maak M, Schuster T, Slotta-Huspenina J, Käser SA, Michalski CW, Janssen KP, Friess H, Rosenberg R, Bader FG. Mucinous and signet-ring cell colorectal cancers differ from classical adenocarcinomas in tumor biology and prognosis. *Ann Surg* 2013; **258**: 775-782; discussion 782-783 [PMID: 23989057 DOI: 10.1097/SLA.0b013e3182a69f7e]

15   **Eisenhauer EA**, Therasse P, Bogaerts J, Schwartz LH, Sargent D, Ford R, Dancey J, Arbuck S, Gwyther S, Mooney M, Rubinstein L, Shankar L, Dodd L, Kaplan R, Lacombe D, Verweij J. New response evaluation criteria in solid tumours: revised RECIST guideline (version 1.1). *Eur J Cancer* 2009; **45**: 228-247 [PMID: 19097774 DOI: 10.1016/j.ejca.2008.10.026]

16   **Delgado AF**, Fahlström M, Nilsson M, Berntsson SG, Zetterling M, Libard S, Alafuzoff I, van Westen D, Lätt J, Smits A, Larsson EM. Diffusion Kurtosis Imaging of Gliomas Grades II and III - A Study of Perilesional Tumor Infiltration, Tumor Grades and Subtypes at Clinical Presentation. *Radiol Oncol* 2017; **51**: 121-129 [PMID: 28740446 DOI: 10.1515/raon-2017-0010]

17   **Gillies RJ**, Kinahan PE, Hricak H. Radiomics: Images Are More than Pictures, They Are Data. *Radiology* 2016; **278**: 563-577 [PMID: 26579733 DOI: 10.1148/radiol.2015151169]

18   **Bowen L**, Xiaojing L. Radiogenomics of Clear Cell Renal Cell Carcinoma: Associations Between mRNA-Based Subtyping and CT Imaging Features. *Acad Radiol* 2019; **26**: e32-e37 [PMID: 30064916 DOI: 10.1016/j.acra.2018.05.002]

19   **Kraemer HC**. Correlation coefficients in medical research: from product moment correlation to the odds ratio. *Stat Methods Med Res* 2006; **15**: 525-545 [PMID: 17260922 DOI: 10.1177/0962280206070650]

20   **van Smeden M**, Moons KG, de Groot JA, Collins GS, Altman DG, Eijkemans MJ, Reitsma JB. Sample size for binary logistic prediction models: Beyond events per variable criteria. *Stat Methods Med Res* 2019; **28**: 2455-2474 [PMID: 29966490 DOI: 10.1177/0962280218784726]

21   **Vittinghoff E**, McCulloch CE. Relaxing the rule of ten events per variable in logistic and Cox regression. *Am J Epidemiol* 2007; **165**: 710-718 [PMID: 17182981 DOI: 10.1093/aje/kwk052]

22   **Baeßler B**, Weiss K, Pinto Dos Santos D. Robustness and Reproducibility of Radiomics in Magnetic Resonance Imaging: A Phantom Study. *Invest Radiol* 2019; **54**: 221-228 [PMID: 30433891 DOI: 10.1097/RLI.0000000000000530]

23   **Ma Y**, Ma W, Xu X, Cao F. How Does the Delta-Radiomics Better Differentiate Pre-Invasive GGNs From Invasive GGNs? *Front Oncol* 2020; **10**: 1017 [PMID: 32766129 DOI:

10.3389/fonc.2020.01017]

24   **Kim HS**, Kim YJ, Kim KG, Park JS. Preoperative CT texture features predict prognosis after curative resection in pancreatic cancer. *Sci Rep* 2019; **9**: 17389 [PMID: 31757989 DOI: 10.1038/s41598-019-53831-w]

25   **Loh HH**, Leu JG. The analysis of natural textures using run length features. *IEEE Trans Indus Elec* 1988; **35**: 323-328 [DOI: 10.1109/41.192665]

26   **Roemeling S**, Roobol MJ, Kattan MW, van der Kwast TH, Steyerberg EW, Schröder FH. Nomogram use for the prediction of indolent prostate cancer: impact on screen-detected populations. *Cancer* 2007; **110**: 2218-2221 [PMID: 17893906 DOI: 10.1002/cncr.23029]

27   **Peeters KC**, Kattan MW, Hartgrink HH, Kranenbarg EK, Karpeh MS, Brennan MF, van de Velde CJ. Validation of a nomogram for predicting disease-specific survival after an R0 resection for gastric carcinoma. *Cancer* 2005; **103**: 702-707 [PMID: 15641033 DOI: 10.1002/cncr.20783]

28   **Kattan MW**, Wheeler TM, Scardino PT. Postoperative nomogram for disease recurrence after radical prostatectomy for prostate cancer. *J Clin Oncol* 1999; **17**: 1499-1507 [PMID: 10334537 DOI: 10.1200/JCO.1999.17.5.1499]

29   **Kouri M**, Pyrhönen S, Kuusela P. Elevated CA19-9 as the most significant prognostic factor in advanced colorectal carcinoma. *J Surg Oncol* 1992; **49**: 78-85 [PMID: 1738240 DOI: 10.1002/jso.2930490204]

30   **Wang WS**, Lin JK, Chiou TJ, Liu JH, Fan FS, Yen CC, Lin TC, Jiang JK, Yang SH, Wang HS, Chen PM. CA19-9 as the most significant prognostic indicator of metastatic colorectal cancer. *Hepatogastroenterology* 2002; **49**: 160-164 [PMID: 11941943]

31   **Zhou W**, Yang F, Peng J, Wang F, Lin Y, Jiang W, Yang X, Li L, Lu Z, Wan D, Pan Z, Fan W. High pretreatment serum CA19-9 level predicts a poor prognosis for patients with stage III colon cancer after curative resection and adjuvant chemotherapy. *J Cancer* 2019; **10**: 3810-3818 [PMID: 31333798 DOI: 10.7150/jca.31375]

32   **Märkl B**. Stage migration *vs* immunology: The lymph node count story in colon cancer. *World J Gastroenterol* 2015; **21**: 12218-12233 [PMID: 26604632 DOI: 10.3748/wjg.v21.i43.12218]